

Published in final edited form as:

Nat Commun. ; 5: 4446. doi:10.1038/ncomms5446.

Host iron status and iron supplementation mediate susceptibility to erythrocytic stage *Plasmodium falciparum*

Martha A. Clark¹, Morgan M. Goheen¹, Anthony Fulford^{2,3}, Andrew M. Prentice^{2,3}, Marwa A. Elnagheeb⁴, Jaymin Patel⁴, Nancy Fisher¹, Steve M. Taylor⁵, Raj S. Kasthuri⁶, and Carla Cerami⁴

¹ Department of Microbiology and Immunology, University of North Carolina, Chapel Hill, North Carolina 27599, USA.

² Medical Research Council International Nutrition Group, London School of Hygiene and Tropical Medicine, London WC1E 7HT, UK.

³ Medical Research Council, Keneba, The Gambia.

⁴ Department of Epidemiology, Gillings School of Global Public Health, University of North Carolina, Chapel Hill, North Carolina 27599, USA.

⁵ Division of Infectious Diseases and International Health, Duke University Medical Center, Durham, North Carolina 27710, USA.

⁶ Division of Hematology Oncology, Department of Medicine, University of North Carolina, Chapel Hill, North Carolina 27599, USA.

Abstract

Iron deficiency and malaria have similar global distributions, and frequently co-exist in pregnant women and young children. Where both conditions are prevalent, iron supplementation is complicated by observations that iron deficiency anaemia protects against falciparum malaria, and that iron supplements increase susceptibility to clinically significant malaria, but the mechanisms remain obscure. Here, using an *in vitro* parasite culture system with erythrocytes from iron-deficient and replete human donors, we demonstrate that *Plasmodium falciparum* infects iron-deficient erythrocytes less efficiently. In addition, owing to merozoite preference for young erythrocytes, iron supplementation of iron-deficient individuals reverses the protective effects of iron deficiency. Our results provide experimental validation of field observations reporting protective effects of iron deficiency and harmful effects of iron administration on human malaria susceptibility. Because recovery from anaemia requires transient reticulocytosis, our findings

© 2014 Macmillan Publishers Limited. All rights reserved.

Correspondence and requests for materials should be addressed to C.C. (ccerami@unc.edu).

Author contributions

M.A.C., M.M.G., C.C., N.F., M.A.E. performed experiments; R.S.K. and C.C. recruited patients; M.A.C., M.M.G., S.M.T., A.F., A.M.P., J.P. and C.C. analysed data; M.A.C., M.M.G., A.M.P., A.F., S.M.T. and C.C. wrote the manuscript.

Supplementary Information accompanies this paper at <http://www.nature.com/naturecommunications>

Competing financial interests: The authors declare no competing financial interests.

How to cite this article: Clark, M. A. et al. Host iron status and iron supplementation mediate susceptibility to erythrocytic stage *Plasmodium falciparum*. Nat. Commun. 5:4446 doi: 10.1038/ncomms5446 (2014).

imply that in malarious regions iron supplementation should be accompanied by effective measures to prevent falciparum malaria.

The interactions between falciparum malaria and iron deficiency anaemia (IDA) are complex and bi-directional. Malaria causes acute anaemia by destroying both infected and uninfected red blood cells (RBCs)¹, whereas persistent sub-clinical infection causes a milder anaemia of infection by blocking iron recycling to the bone marrow². Conversely, once established, IDA protects both pregnant women³⁻⁵ and children⁶⁻⁸ from malaria. In addition, supplemental iron, given alone or in combination with other micronutrients, predisposes children to malaria^{8,9} and other serious adverse outcomes¹⁰. Iron homeostasis has been implicated in regulating liver stage *P. falciparum* infection; in murine studies, erythrocytic stage malaria infection initiates hepcidin-mediated hepatic hypoferremia, which blocks superinfections by sporozoites from competing plasmodial strains¹¹. Mathematical modelling suggests that this can explain the low levels of superinfections in young children¹¹, but this mechanism cannot account for observed reductions in the risk of primary malaria infection in children with IDA. It has also been speculated that transient peaks in nontransferrin-bound iron caused by administration of highly absorbable iron supplements¹² could promote intra-erythrocytic parasite growth¹³ or bacterial septicemia (a common cause of death in malaria patients¹⁴⁻¹⁶) but definitive evidence is absent.

As iron deficiency and iron supplementation of iron deficient individuals profoundly alters erythropoiesis, RBC physiology, and RBC population structure, we hypothesized that iron deficiency and iron supplementation directly impact the disease causing erythrocytic stage of *P. falciparum* infection. In our investigations, we minimize the confounding factors that have complicated prior field studies of the relationship between host iron status, iron supplementation and falciparum malaria by utilizing an *in vitro* system with freshly isolated RBCs from donors with well-defined, physiologic iron states recruited through our US-based hospital clinic. This approach eliminated the influence of acquired and innate immunity to malaria, haemoglobinopathies and concurrent inflammation. Our study reveals that RBCs from donors with IDA confer malaria protection by impairing *P. falciparum* invasion and intra-erythrocyte propagation. This protective effect was reversed when donors with IDA received iron supplementation. We go on to show that when iron-deficient RBCs are replaced with iron-replete (IR) RBCs *in vitro* (as occurs in individuals with IDA following iron supplementation) the susceptibility to *P. falciparum* infection is increased. These findings support well-described clinical patterns of differential susceptibility to malaria. Taken together, they indicate that therapeutic iron supplementation conspires with host iron status to mediate host RBC susceptibility to malaria infection by altering the dynamic structure of the host's RBC population.

Results

Malaria growth is reduced in RBCs from individuals with IDA

To determine the effect of IDA on the growth of erythrocytic stage *P. falciparum*, we enrolled donors with and without IDA from a non-malaria endemic area through our US-based hospital clinic. Donors were classified as IR (haemoglobin (Hgb) >11 g dl⁻¹, mean

corpuscular volume (MCV) >80 fL, ferritin >12 ng ml⁻¹) or as IDA (Hgb <11 g dl⁻¹, MCV <80 fL, ferritin <12 ng ml⁻¹) (Table 1). Non-anaemic donors with low-iron stores (Hgb >11 g dl⁻¹, ferritin <12 ng ml⁻¹) were excluded. *P. falciparum* (strains 3D7, Dd2 and FCR3-FMG) were grown in either RBCs from the IR ($n = 10$) or IDA ($n = 7$) donors in up to three consecutive 96 h growth assays (Supplementary Fig. 1). We observed that parasite growth rates were reduced in RBCs from IDA donors as compared with growth in RBCs from IR donors by 48.8% (standard deviation (s.d.)±23.9), 34.3% (s.d.±22.2) and 50.0% (s.d.±20.4) for strains 3D7, Dd2 and FCR3-FMG, respectively (Fig. 1a). These findings clearly show that *P. falciparum* propagation is reduced within RBCs from IDA individuals, but that variability may exist in the degree to which different *P. falciparum* isolates are affected by IDA.

Malaria growth is increased in RBCs from iron-supplemented donors

Given field evidence that supplementation of children with 12.5 mg of iron (1–1.5 mg kg⁻¹) and 50 ng of folic acid may potentiate the risk of malaria⁹, we next investigated the effects of iron supplementation of IDA and IR individuals on *in vitro* growth of erythrocytic stage *P. falciparum*. We first collected RBCs from IDA patients who were receiving iron supplementation (IDA + Fe); these individuals met the above criteria for IDA and were receiving either high-dose oral ferrous sulfate (60 mg elemental iron orally three times per day (9–12.6 mg kg⁻¹)) or intravenous iron (at a dosage determined by their personal physician using the following equation: Dose = 0.0442 [desired Hgb—observed Hgb] × LBW + [0.26 × LBW]). IDA + Fe group Hgb values ranged from 6.6 to 9.8 g dL⁻¹ and MCV values ranged from 75 to 98 fL. Additionally reticulocyte counts and red cell distribution width (RDW) were elevated; and average mean corpuscular haemoglobin concentration (MCHC), total iron, and ferritin values were greater than that of the IDA group but still lower than that of the IR group (Table 1). Together, these values are indicative of an erythropoietic response to iron supplements, but not full recovery from IDA. Comparison of the growth rate of *P. falciparum* (strains 3D7, Dd2 and FCR3-FMG) within RBCs from the IDA + Fe donors to the growth rate of parasites within RBCs from IR donors revealed increases in *P. falciparum* growth of 17.3% (s.d.±22.7), 17.6% (s.d.±14.0) and 26.3% (s.d.±16.1) for 3D7, Dd2 and FCR3-FMG in RBCs from IDA + Fe donors (Fig. 1b).

We additionally assessed the effect of iron supplementation of IR individuals on *P. falciparum* growth. For this study, IR individuals donated blood at enrollment (baseline) and were then prescribed daily oral iron supplementation (325 mg ferrous sulfate). Iron-supplemented IR study participants (IR + Fe) subsequently returned at one and two months following initiation of daily iron supplementation to donate blood. At each donation (enrollment, 1 month and 2 months), the growth rate of *P. falciparum* (strains 3D7, Dd2 and FCR3-FMG) within RBCs from IR + Fe donors was determined and then compared with the corresponding parasite growth rates within RBCs from a non-supplemented IR donor. Compared with RBCs from IR donors, we observed in RBCs from IR + Fe donors that 1 month of iron supplementation increases of 17.5% (s.d.±16.1), 11.3% (s.d.±15.7) and 6.6% (s.d.±8.1) in growth for 3D7, Dd2 and FCR3-FMG, respectively. There was no change in parasite growth rate in RBCs collected 1 and 2 months after administering iron supplements (Fig. 1c). Analyses of Hgb, haematocrit, MCV, MCHC, transferrin saturation, ferritin and

reticulocyte count of IR + Fe donors revealed no significant change in their iron status following iron supplementation (Table 1).

To comprehensively compare and ultimately quantify the impact of IDA and iron supplementation on the growth of *P. falciparum* *in vitro*, we integrated data from all growth experiments and fit a multilevel random effects model to the pooled data (Fig. 1d). The outputs of this analysis were growth rates of any parasite strain in experimental RBCs plotted against the growth rate in IR RBC controls. Values were adjusted for variation between study participants, day-to-day differences in parasite preparations and differences in *P. falciparum* strain growth rates. The $Y = X$ line was fit to the growth rate of *P. falciparum* in RBCs from IR donors. Data above the $Y = X$ line indicate growth rates greater than that of parasite growth in RBCs from IR donors and data below the $Y = X$ line indicate growth rates lower than that of parasite growth in RBCs from IR donors. Based on this analysis, we estimate that compared with IR RBCs, *P. falciparum* growth is reduced (59.8% (95% confidence interval (CI) = 51.9–68.8)) in RBCs from IDA donors, and that there is a slight increase in the growth of *P. falciparum* in RBCs from IDA + Fe donors (22.8% (95% CI = 2.7–46.7)) and RBCs from IR + Fe donors (18.9% (95% CI = 5.0–33.9)); no difference was observed between *P. falciparum* growth in RBCs from IR + Fe donors and IDA + Fe donors (Fig. 1e). These data clearly indicate that IDA substantially attenuates the growth of *P. falciparum* parasites and that iron supplementation of donors with IDA reverses the protection provided by IDA against falciparum infection. Furthermore, these data suggest that iron supplementation of IR individuals may slightly increase propagation of erythrocytic stage *P. falciparum*.

RBCs from donors with IDA are refractory to malaria infection

Propagation of the erythrocytic stage of *P. falciparum* may be impeded at the point of (i) invasion, (ii) maturation or (iii) production of infectious daughter merozoites. To determine why *P. falciparum* infection of RBCs from IDA donors is reduced, we systematically assessed the capacity of *P. falciparum* to progress through each of these rate-limiting steps within RBCs from IDA donors compared with RBCs from IR donors. To assess invasion, we directly compare invasion of *P. falciparum* strains 3D7, Dd2 and FCR3-FMG into RBCs from IDA and IR donors with a barcoded RBC flow cytometry based invasion assay. To express the differential invasion of RBCs, we computed the susceptibility index (SI), which is the ratio of the relative risk of invasion of RBCs from IDA donors to that of RBCs from IR donors. An SI of 1.0 indicates no difference in parasite invasion between two RBC populations. In experiments with strains 3D7, Dd2 and FCR3-FMG, the mean SI of RBCs from IDA donors relative to RBCs from IR donors was 0.56 (95% CI = 0.56–0.57), 0.52 (95% CI = 0.52–0.53) and 0.70 (95% CI = 0.69–0.71), respectively, indicating consistently reduced invasion of RBCs from IDA donors (Fig. 2a). We next assessed parasite maturation within RBCs from IDA donors by analysing Giemsa-stained thin blood smears, which were made every 6 h during the course of a 48-h intra-erythrocytic lifecycle. We observed that parasites matured normally in iron-deficient RBCs, indicating that the reduced overall parasite growth in iron-deficient RBCs did not result from delayed maturation (Fig 2b,c). Finally, we measured the parasitized erythrocyte multiplication rate (PEMR)^{17,18} of *P. falciparum* within RBCs from IDA donors as compared with RBCs from IR donors. For

parasite strains 3D7, Dd2 and FCR3-FMG, RBCs from IDA donors (relative to RBCs from IR donors) had a reduced PEMR of 48.0% (s.d.±12.2), 25.7% (s.d.±2.2) and 39.9% (s.d.±9.3), respectively (Fig. 2d). In accordance with the PEMR data, we additionally observed fewer merozoites within IDA as compared with IR RBCs by microscopy (data not shown). Taken together, these data indicate that *P. falciparum* matures normally within RBCs from IDA donors, but that invasion into and production of infectious merozoites within RBCs from IDA donors are significantly reduced. These data additionally reveal that different *P. falciparum* isolates may exhibit different invasion and PEMR phenotypes in RBCs of IDA individuals.

Replacement of iron-deficient RBCs increases malaria growth

The erythropoietic rate of iron-deficient individuals increases dramatically in response to iron supplementation, and elevated erythropoietic rate is hypothesized to increase an individual's susceptibility to malaria¹⁹. As the iron biomarkers of individuals in the IDA + Fe group were indicative of an erythropoietic response to iron (Table 1), we hypothesized that the replacement of iron-deficient RBCs with IR RBCs would explain the recovered growth of *P. falciparum* in RBCs from IDA + Fe donors (Fig. 1). To determine whether the replacement of iron-deficient RBCs with young IR RBCs could explain the recovered growth of *P. falciparum* in RBCs donated by IDA + Fe individuals, we first compared *P. falciparum* infection of reticulocytes (CD71+) and mature RBCs (CD71-) from IDA + Fe donors. Consistent with *P. falciparum*'s reported preference for young RBCs, we observed 8.6% (s.d.±0.1) parasitization of reticulocytes (CD71+) and 4.5% (s.d.±0.4) parasitization of mature RBCs (CD71-)(Fig. 3a). However, (CD71 +) reticulocytes accounted for only 1.6% (s.d.±0.9) of all RBCs and parasitized (CD71+) reticulocytes only contributed to 3.0% (s.d.±0.1) of the total number of parasitized RBCs (Fig. 3b).

Having clearly demonstrated that reticulocytes from IDA Fe donors are more highly infected by *P. falciparum*, but +that reticulocytes themselves only contribute marginally to the total infection, we next sought to definitively determine whether the replacement of iron-deficient with IR RBCs could explain the recovered growth of *P. falciparum* in RBCs from IDA Fe donors. However, low incidence of IDA in our study setting,+the difficulty of following iron-supplemented IDA individuals longitudinally through full recovery from iron deficiency, as well as the inability to use the common surrogates of RBC age (volume and density) against the background of changing host iron status, prevented us from studying the impact of an elevated erythropoietic rate on erythrocytic stage *P. falciparum* infection. Therefore, we modelled the effect of iron supplementation-mediated changes in RBC population dynamics on erythrocytic stage *P. falciparum* infection by assessing the impact of replacing RBCs from IDA donors with RBCs from IR donors on *in vitro P. falciparum* growth. Replacing 10, 25, 50 and 75% of the RBCs from IDA donors with RBCs from IR donors resulted in a steady increase in parasite growth rate; 75% replacement recovered 3D7, Dd2 and FCR3-FMG *P. falciparum* growth rate to 88.2% (s.d.±2.0), 89.7% (s.d.±2.5) and 92.3% (s.d.±1.1) that of the growth rate of in RBCs from IR donors, respectively (Fig. 3c).

As the first step in the erythrocytic life cycle of the malaria parasite, erythrocyte invasion is a pivotal determinant of the magnitude of infection. Therefore, we utilized the barcoded RBC invasion assay to determine how iron-deficient and IR RBCs interact to shape *P. falciparum* invasion. Like growth rate, *P. falciparum* invasion rate increased as IDA RBCs were replaced with IR RBCs. Rate of invasion was fully recovered to IR levels once 80% of IDA RBCs were replaced with IR RBCs for all three parasite strains (Fig. 3d and Supplementary Fig. 2a). Furthermore, employment of the barcoded RBC invasion assay allowed for the full characterization of the kinetics of *P. falciparum* invasion into IDA and IR RBCs, as the frequency of each changed relative to the total RBC population. We observed that the number of *P. falciparum* FCR3-FMG invasions into IDA and IR RBCs increased linearly, as each RBC population increased in frequency, $R^2 = 0.984$ and 0.931 , respectively, and *P. falciparum* invasion as a function of IDA RBC abundance was significantly less than that of IR RBCs (Fig. 3e). Similar trends were observed for *P. falciparum* strains 3D7 and Dd2 (Supplementary Fig. 2b and c). Together, these results support the hypothesis that replacing an individual's iron-deficient RBC population with IR RBCs would increase the host's susceptibility to erythrocytic stage *P. falciparum* infection and clearly illustrate the impact RBC population dynamics have on potential parasite biomass and pathogenesis. Moreover, our use of the barcoded RBC invasion assay allowed for the definitive determination and characterization of the distribution of parasites in IDA and IR RBC populations, as the frequency of each changed.

Effect of RBC population age structure on malaria infection

Reticulocytes and young RBCs are preferentially invaded by *P. falciparum*^{20,21}, and theoretical models predict that elevated reticulocytosis may increase the risk of high parasite density^{19,22}. Because of the shortened lifespan of iron-deficient RBCs, there is a period in the course of an individual's recovery from IDA at which point protective iron-deficient RBCs have been cleared from circulation and the remaining circulating RBCs are on average younger than that of an IR individual. To determine the capacity of young RBCs to shape *P. falciparum* infection, we (i) directly compare *P. falciparum* infection of young RBCs and RBCs of increasing age and (ii) model the effect of replacing young IR RBCs with old IR RBCs on *P. falciparum* growth and invasion *in vitro*. For these studies, we utilized two proxies for RBC age: RBC volume, which decreases with age²³ and is unaffected by ring stage parasitization²⁴, and RBC density, which increases with increasing RBC age²³. We observed that when RBCs from an IR donor were infected with *P. falciparum*, parasite infection increased with increasing RBC volume (Fig. 4a). To directly compare *P. falciparum* invasion of RBCs of different ages, we density separated RBCs from IR donors into four fractions of increasing RBC age: young, young adult, mature adult and old (Supplementary Fig. 3A). Decreasing MCV, reticulocyte content and Calcein fluorescence²⁵ confirmed the age separation of the RBCs (Supplementary Fig. 3b–d). We observed that the SI of young adult, mature adult and old RBCs to parasite invasion as compared with young RBCs was 0.85 (95% CI = 0.82–0.90), 0.58 (95% CI = 0.56–0.62) and 0.28 (95% CI = 0.27–0.30), respectively (Fig. 4b). In accordance with previous reports^{17,20,26}, young RBCs sustained a significantly greater growth rate than young adult, mature adult and old RBCs, with young RBCs supporting a growth rate 50% greater than old RBCs (Supplementary Fig. 3e), and compared with young RBCs the PEMR was reduced

by 10% (s.d. \pm 4.78), 15% (s.d. \pm 1.16) and 19% (s.d. \pm 2.23) in young adult, mature adult and old RBCs, respectively (Supplementary Fig. 3f). These data clearly demonstrate the preferential invasion of *P. falciparum* into young RBCs and show that the risk of RBCs to *P. falciparum* invasion relative to young RBCs decreases with increasing RBC age. All together we have confirmed (i) *P. falciparum* infection is more prevalent in young RBCs (ii) the increased capacity of young RBCs to support *P. falciparum* invasion and growth.

To determine the capacity of the age distribution of a RBC population to shape *P. falciparum* infection, we examined the effect of replacing young IR RBCs with old IR RBCs on *P. falciparum* growth *in vitro*. We observed 15.7% (s.d. \pm 3.1) greater growth of *P. falciparum* in young IR RBCs as compared with density separated and then recombined (total) IR RBCs, and growth remained significantly greater when 10% of young RBCs were replaced with old RBCs. Following replacement of 33, 50, 66, 80 and 90% of young RBCs with old RBCs, *P. falciparum* growth rate steadily decreased (Fig. 4c). Consistent with *P. falciparum* growth, we observe that the rate of *P. falciparum* invasion into young RBCs is significantly greater than that of total IR RBCs (29.0% (s.d. \pm 2.1)). Furthermore, we observed that as the frequency of young RBCs decreased from 100 to 50% and the frequency of old RBCs increased from 0 to 50%, the total rate of invasion decreased by only 4.9% (s.d. \pm 0.7), maintaining a *P. falciparum* invasion rate significantly greater than that of the invasion rate of total RBCs. However, when the frequency of young RBCs fell from 50 to 0% and old RBCs increased from 50 to 100%, *P. falciparum* infection decreased steadily, ultimately falling by 45.7% (s.d. \pm 1.9) (Fig. 4d).

As young IR RBCs are at the greatest risk of *P. falciparum* invasion, we speculated that an insufficient merozoite inoculum might be responsible for the observed plateau in *P. falciparum* invasion. However, invasion experiments with double the inoculum of merozoites also resulted in a plateau in the rate of *P. falciparum* invasion when young RBCs accounted for more than 50% of the total RBCs population (Supplementary Fig. 4a). Moreover, the rate of *P. falciparum* invasion achieved with the higher inoculum was less than that of the lower inoculum invasion experiments (Fig. 4d and Supplementary Fig. 4a). We subsequently characterized the kinetics of *P. falciparum* invasion into young and old RBCs as the frequency of each changed relative to the total RBC population. We observed that like *P. falciparum* invasion of IDA and IR RBCs, the number of *P. falciparum* invasions into old IR RBCs increased linearly as old IR RBCs increased in frequency, $R^2 = 0.991$. In contrast, the number of *P. falciparum* invasions into young IR RBCs as a function of young IR RBC abundance was best fit by a logarithmic function, $R^2 = 0.976$ (Fig. 4e). The same kinetics of *P. falciparum* invasion were observed when experiments were performed with double the merozoite inoculum (Supplementary Fig. 4b). These results demonstrate that replacement of young IR RBCs with old IR RBCs reverses the elevated growth and invasion rate sustained by young IR RBCs. In addition, we show that the rate of *P. falciparum* invasion only begins to dramatically drop off once 50% of young IR RBCs have been replaced with old IR RBCs, and that this can be attributed to the logarithmic nature of *P. falciparum* invasion of young IR RBCs. Together, these data support the hypothesis that the effects of iron deficiency and iron supplementation on RBC physiology

and erythropoietic rate are at least partially responsible for determining an individual's risk of malaria infection (Fig. 5).

Discussion

Iron supplementation has clear nutritional benefits for children and pregnant women², but iron is also an essential nutrient for most pathogens and as a result is a critical mediator of host–pathogen interactions²⁷. Activation of the host innate immune system by the malaria parasite or other infectious organisms triggers reduction in iron absorption, redistribution of existing iron stores and decreases erythropoiesis, which effectively limits the availability of iron to invading pathogens. It is unknown what host iron (mosquito or human) *P. falciparum* is able to access and utilize nor how the parasite circumvents the host's attempt to restrict iron. It has been previously postulated that as occurs with other pathogens²⁸, iron deficiency inhibits *P. falciparum* infection via iron deprivation. Although the malaria parasite may find iron less readily available in an iron-deficient host, our work reveals an alternate cellular mechanism by which iron deficiency may protect against malaria. Our study of the relationship between iron deficiency, iron supplementation and erythrocytic stage *P. falciparum* infection highlights how by altering the dynamics of the human hosts RBC population iron deficiency and iron supplementation shape erythrocytic stage *P. falciparum* infection.

Clinical studies in different field sites have reported that iron deficiency correlates with protection from malaria. In Malawian children, baseline iron deficiency was associated with significant reductions in the subsequent risks of both parasitemia (45%) and malaria (51%)²⁹. Similarly, in Tanzanian children, baseline iron deficiency significantly decreased the odds of subsequent parasitemia (23%) and severe malaria (38%)⁶. In addition, in two studies of pregnant women, iron deficiency was associated with a decreased prevalence of placental malaria, a major cause of neonatal and maternal morbidity^{3,4}. Our results—that iron-deficient RBCs impair parasite propagation *in vitro* (Fig. 1)—are consistent with these clinical findings, and provide valuable insight into a cellular mechanism for the observations made in the clinical setting. In our study of *P. falciparum* growth in RBCs from IDA donors, we reveal that RBCs from IDA donors are refractory to *P. falciparum* invasion and support a lower PEMR but that parasite maturation is normal (Fig. 2). There are multiple physiological differences between iron-deficient and IR RBCs that may contribute to the impaired invasion into and replication within iron-deficient RBCs. These include greater osmotic fragility and membrane rigidity, accelerated ageing *in vivo*^{30–33}, lower Hgb content and smaller size (microcytosis).

Iron supplementation has long been hypothesized to increase malaria risk, and this issue has garnered recent attention after a large-scale nutritional supplementation study in Tanzanian children was halted owing to significantly increased mortality among those receiving iron⁸. Although it remains unclear whether the increased mortality rate was secondary to malaria, this potential for harm has complicated recommendations for widespread supplementation and has caused iron supplementation programmes in malaria endemic countries to be suspended. In a more recent randomized trial of Tanzanian children, iron supplementation increased the risk of malaria by 41% in iron-deficient but not in IR children⁸. Notably, our

studies are consistent with the Tanzania study. Specifically, we observed increased parasite growth in RBCs donated by iron-supplemented IDA individuals and a modest effect in RBCs donated by iron-supplemented IR individuals (Fig. 1). As individuals in the iron-supplemented IDA group were observed to be undergoing an erythropoietic response to iron supplementation (Table 1), we proceeded to investigate the effect of replacing iron-deficient RBCs with IR RBCs and young RBCs with old RBCs on *P. falciparum* erythrocyte infection. We demonstrate that *P. falciparum* growth and invasion rates increase when iron-deficient RBCs are replaced with IR RBCs (Fig. 3). Furthermore, we show that young RBCs support greater *P. falciparum* growth and invasion rates than total IR RBCs and that the replacement of young RBCs with old RBCs reverses the effect of young RBCs on parasite growth and invasion (Fig. 4). Finally, in the course of these experiments, our use of barcoded RBC flow cytometry invasion assay has provided novel insight into the relationship between the frequency of a RBC subset in the total RBC population and *P. falciparum* infection (Figs 3e and 4e). In summary, our results demonstrate that the changes in the RBC population that occur during recovery from IDA enhance parasite propagation.

It should be noted that our work exclusively focuses on the influence of iron deficiency and iron supplementation on the susceptibility of the human host's RBC to malaria infection, and does not address the potential effect of serum iron¹³ or additional factors, which may function in vivo, including growth of the hepatic stage of the parasite³⁴, rosetting and cytoadherence to the endothelium, accelerated clearance of parasitized RBCs^{35,36}, effects of innate immune factors such as hepcidin¹¹ and lipocalin 2 (ref. 37), or adaptive immune function. We have previously reported that both transferrin and ferric citrate increase the bioavailable iron pool of trophozoite-infected RBCs but not that of uninfected RBCs¹³. It is possible that parasite growth may be enhanced by the transient increase in serum iron that is observed in IR individuals who are given oral iron supplementation¹². Further investigations need to be conducted to explore the extent to which iron deficiency and iron supplementation shape other aspects of malaria pathogenesis.

Our findings, taken together with those from field studies, raise the important medical and public health question: How can iron supplementation be safely administered to IDA children in malarious areas? A critical implication of these observations is that reconstitution of red cell mass in anaemic patients would be expected to transiently enhance susceptibility to malaria (Fig. 5), which may inform the on-going debate as to whether fortification with iron would be safer than supplemental iron. Our data implies that, where *P. falciparum* is endemic, treatment of anaemia with iron supplementation should be accompanied by malaria preventive measures, such as malaria prophylaxis, bed nets and increased active surveillance and access to health care. Additional questions raised by this study are: Does iron deficiency in African children represent an evolutionarily advantageous phenotype that derives from polymorphisms in iron homeostasis? What molecular mechanisms confer protection from malaria in the setting of microcytosis, and can these protective mechanisms be exploited by medical interventions? Future clinical and translational studies will be needed in order to design safe and effective interventions to address the twin burdens of iron deficiency and falciparum malaria.

Methods

Clinical

Study participants included healthy, HIV-negative, non-pregnant donors over 18 years of age with and without IDA. Exclusion criteria included: on-going inflammation or infection, previous history of malaria, travel to malaria endemic areas, malignancy, sickle cell disease (or trait), thalassemia (or trait for either thalassemia- α or - β). This study was approved by the University of North Carolina Institutional Review Board, Protocol # 09-0559, and informed consent was obtained from all subjects. Study participants with Hgb >11 g dl⁻¹ and ferritin >12 ng ml⁻¹ were classified as IR and participants with Hgb <11 g dl⁻¹ and ferritin <12 ng ml⁻¹ were classified as IDA. IDA + Fe donors were identified by their personal physicians for participation in our study. Subjects were included in the IDA + Fe group if they fit the criteria for IDA and had been prescribed high-dose oral ferrous sulfate, 60 mg (9–12.6 mg kg⁻¹) elemental iron orally three times per day or intravenous iron at a dosage determined by their personal physician sulfate once daily using the following equation: Dose = 0.0442 [desired Hgb observed Hgb] \times LBW + [0.26 \times LBW]. Healthy donors took 325 mg of ferrous sulfate once daily for the 2-month duration of the study. These donors donated 40 ml of blood on three occasions— at enrollment and two subsequent monthly intervals. An additional group of healthy donors served as the IR control group. Non-anaemic donors with low-iron stores (Hgb >11 g dl⁻¹, ferritin <12 ng ml⁻¹) were excluded. Full iron panels were obtained for each study participant and mean values for each group are reported in Table 1.

Parasite culture

P. falciparum parasite strains 3D7, Dd2 and FCR3-FMG were cultured in RBCs from O +, IR donors at 2–3% haematocrit and Albumax Complete Media (ACM)–RPMI 1640 (Sigma-Aldrich) with 10% AlbuMAX II (Gibco), 1 mM hypoxanthine (Sigma-Aldrich), 20 mM L-glutamine (Cellgro), 0.45% glucose (Cellgro) and 0.01 ng ml⁻¹ gentamicin (Sigma-Aldrich). AlbuMAX II was used to supplement the media in place of human serum to isolate the effects of the RBCs from different experimental groups. All RBCs used for parasite culture were obtained from well-characterized IR O + donors and used within 14 days of being drawn. Cultured parasites were maintained between 0.5 and 10% at 37 °C, in an atmosphere of 5% O₂, 5% CO₂ and 90% N₂ with continuous shaking. Early ring stage parasites were synchronized with 5% (w/v) D-sorbitol. Synchronization was repeated at 20 and 40 h to achieve a tightly synchronized parasite population.

Growth assay

P. falciparum parasites from routine cultures were seeded as rings at 0.5% initial parasitemia in 1% haematocrit in ACM in triplicate in 96-well plates. Parasites were maintained for 96 h under standard culture conditions and the media was changed daily. At 96 h, parasite cultures were split back to 0.5% parasitemia and maintained as described for an additional 96 h (Supplementary Fig. 1). Parasites were stained at all 0 and 96 h time points with 1 \times DNA dye SYBR Green I (Invitrogen) as described in ref. 38, and fixed in 1% paraformaldehyde and 0.0075% glutaraldehyde (Electron Microscopy Sciences) in Alsever's Solution (Sigma-Aldrich) for 30 min at 4 °C. Fixative was removed and cells were stored in

PBS at 4 °C until analysis by flow cytometry. Growth rate reflects the fold increase in RBC parasitization between 0 and 96 h. To identify parasitized reticulocytes, cultures were stained with 0.5 µM DNA dye SYTO 61 (Invitrogen)^{13,39} and PE-conjugated mouse anti-human CD71 antibody (Miltenyi Biotech) and analysed by flow cytometry.

Barcoded RBC invasion assay

RBCs were labelled with 5 mM of either CellTrace Violet or CellTrace Far Red DDAO-SE (Invitrogen) as described³⁹. Violet- and DDAO-labelled RBCs were combined in ACM and delivered in triplicate into 96-well plates and subsequently seeded with schizonts to achieve 1.5–2% parasitized RBCs. Parasites were maintained for 12–18 h under standard culture conditions to allow for schizont rupture and subsequent invasion of CellTrace-labelled RBCs. The invasion of *P. falciparum* into Violet- and DDAO-labelled RBCs was directly compared by measuring the SI, defined as the ratio of the prevalences of infected Violet RBCs to infected DDAO RBCs⁴⁰. Note that the SI is different from the previously described selectivity index^{18,41}. The selectivity index has been used to report the number of multiply infected cells, whereas the SI defines the relative susceptibility to invasion of two different types of RBCs.

Parasite erythrocyte multiplication rate assay

Trophozoite-infected cultures were magnetic activated cell sorting (MACS) purified and seeded into experimental RBCs to achieve 1.5–2% pRBCs and incubated for 48 h to allow for invasion of merozoites into experimental RBCs and their subsequent development into trophozoites inside the experimental RBCs. Experimental RBC parasite density was determined and the same number of infected experimental RBCs was seeded into separate wells containing target RBCs (from an IR donor) to achieve 1.5–2% pRBCs. Cultures were then incubated for 12–18 h to allow merozoites produced within experimental RBCs to invade target RBCs, allowing for assessment of the PEMR^{17,18}. Following invasion of target RBCs, cells were stained with SYBR Green I and analysed by flow cytometry to determine the total number of ring pRBCs. PEMR reflects the number of merozoite invasions of target RBCs per schizont infected experimental RBC.

Density separation

RBCs were separated into five fractions with a modified version of previously described density gradient centrifugation method²³. Briefly, blood was collected into acid citrate dextrose and plasma was subsequently removed by centrifugation for 15 min at 800g. Packed cells were resuspended at 50% haematocrit in RPMI, and passed over a 2:1 (w/w) α -cellulose/microcrystalline cellulose column to remove lymphocytes⁴². Following lymphocyte depletion, RBCs were washed twice with RBC buffer (10 mM HEPES, 12 mM NaCl, 115 mM KCl, 5% BSA). RBCs were layered onto a 65, 60, 55 and 50% discontinuous Percoll gradient and then centrifuged for 25 min at 1,075 g. Each of the five fractions was removed, washed twice with RBC buffer and stored at 4 °C for up to 5 days. Decreasing MCV, reticulocyte content and Calcein fluorescence²⁵ of the five fractions confirmed the age separation of RBCs (Supplementary Fig. 3c–g). For barcoded RBC invasion assays and

growth assays, which utilized density separated RBCs, recombined RBCs were included as a 'total' RBC control.

Flow cytometry

Growth, invasion and infectious merozoite production assays were analysed by flow cytometry using either a modified FACS-Calibur with two lasers 30 mW 488 Diode Pumped Solid State laser and a 25-mW 637 red diode laser (FACS-Calibur; Becton Dickinson, modified by Cytex Development) or a Beckman-Coulter (Dako) CyAn ADP. Channels and probes used on the FACSCalibur included: SYTO 61 (637 nM, 666/27 bandpass), PE (488 nM, 585/42 bandpass) and SYBR Green I (488 nM, 530/30 bandpass). FACS-Calibur data were collected using FlowJo CE and analysed with Summit v5.1. Channels and probes used on the Dako cyan included: CellTrace Violet (405 nM, 450/50 bandpass), SYBR Green I (488 nM, 530/40 bandpass) and CellTrace DDAO-SE (635 nM, 665/20 bandpass). Data from the Cyan cytometer were collected and analysed with Summit v4.3.01. Linear amplification of forward scatter was used to set event threshold in order to exclude cell debris, microparticles and doublets. Electronic volume of uninfected RBCs and pRBCs was assessed on a Beckman Coulter Cell lab Quanta (Beckman Coulter). Channels and probes used on the Quanta included: SYBR Green I (488 nM, 525/40 bandpass). National Institute of Standards and Technologies-certified beads standard L2 2 μm , L5 5 μm and L10 10 μm (Beckman Coulter) were used to calibrate electronic volume. Calibrated data were expressed as both electronic volume (μm^3) and diameter (μm). Quanta data were collected with Cell Lab Quanta Collection Software for Instrument Control and analysed with Kaluza (Beckman Coulter). For all experiments, samples were diluted to 0.001–0.002% haematocrit and 100,000–500,000 total events were collected.

Statistical methods

All experiments were performed in triplicate. Results are from either one representative experiment or the combined results of at least three independent experiments. Parasite growth rate and infectious merozoite production experiments were analysed with two-tailed Student's *t*-test and one-way analysis of variance (GraphPad Prism 5).

Data from all *in vitro* growth studies were pooled and analysed using random effects regression (Fig. 1d,e). The dependent variable in the analysis was the logarithm of the ratio of the percent pRBCs at 96 h (final) and 0 h (initial). In addition, to the usual variation independently affecting each observation, we fitted two higher levels of variance: variation between individuals and day-to-day variation in parasite 'preparations' taking account of the fact that in this data set these two variance components were cross (rather than the more usually encountered nested design). We fitted two exposure variables, iron status and iron supplementation, both as binary variables, and their interaction, focusing on three contrasts: supplemented IDA versus supplemented IR donors; supplemented versus non-supplemented IDA donors; supplemented versus non-supplemented IR donors. All experiments were performed in triplicate with three *P. falciparum* strains (3D7, Dd2 and FCR3-FMG) and consisted of three serial 96 h growth assays (Supplementary Fig. 1); *P. falciparum* strain, growth assay number and their (highly significant) interaction were fitted as binary covariates. We noted that when 0 h (initial) percent pRBCs was greater than 1, the second

growth assay always gave anomalous low results (most likely due to a saturation effect). As these data were uninformative and yet added noise to the analysis, we omitted all such cases while noting that although their inclusion increased the standard errors, it did not change the same general conclusions of the analysis. This model was fitted using Stata's xtmixed procedure (v12, Stata Corp).

To compare the susceptibility of different RBC types to invasion by *P. falciparum*, an unadjusted odds ratio was used to calculate the SI. All statistical analyses for invasion experiments were performed with Stata/IC (v10, Stata Corp). Linear regression was employed to investigate the associations between host iron status and parasite invasion *in vitro* using percent of RBCs from IDA or IR donors as the independent variable and total invasions/ 1×10^5 RBCs as the dependent variable (Fig. 3e). Analysis of covariance was conducted to determine whether the invasion into the two groups were the same. An α of 0.05 was set a priori to determine statistically significant differences. Similar analysis was done to better understand associations between RBC age and parasite invasion (Fig. 4e).

Supplementary Material

Refer to Web version on PubMed Central for supplementary material.

Acknowledgments

We gratefully acknowledge the individual donors who participated in the study. We also thank Michael Nicholson of Precision Biosciences for the use of the Beckman Quanta Flow cytometer and Steven R. Meshnick for critically reading the manuscript. The work was supported by the National Institute of Child Health and Human Development under award number U01HD061235 (to C.C.). The UNC Flow Cytometry Core Facility is supported in part by an NCI Center Core Grant number P30CA06086. S.M.T. is supported by the National Institute of Allergy and Infectious Diseases under award number K08AI100924.

References

1. Price RN, et al. Factors contributing to anemia after uncomplicated falciparum malaria. *Am. J. Trop. Med. Hyg.* 2001; 65:614–622. [PubMed: 11716124]
2. Nweneka CV, Doherty CP, Cox S, Prentice A. Iron delocalisation in the pathogenesis of malarial anaemia. *Trans. R. Soc. Trop. Med. Hyg.* 2010; 104:175–184. [PubMed: 19783267]
3. Kabyemela ER, Fried M, Kurtis JD, Mutabingwa TK, Duffy PE. Decreased susceptibility to *Plasmodium falciparum* infection in pregnant women with iron deficiency. *J. Infect. Dis.* 2008; 198:163–166. [PubMed: 18500927]
4. Senga EL, Harper G, Koshy G, Kazembe PN, Brabin BJ. Reduced risk for placental malaria in iron deficient women. *Malar. J.* 2011; 10:47. [PubMed: 21345193]
5. Sangaré L, van Eijk AM, Ter Kuile FO, Walson J, Stergachis A. The association between malaria and iron status or supplementation in pregnancy: a systematic review and meta-analysis. *PLoS ONE.* 2014; 9:e87743. [PubMed: 24551064]
6. Gwamaka M, et al. Iron deficiency protects against severe *Plasmodium falciparum* malaria and death in young children. *Clin. Infect. Dis.* 2012; 54:1137–1144. [PubMed: 22354919]
7. Nyakeriga AM, et al. Iron deficiency and malaria among children living on the coast of Kenya. *J. Infect. Dis.* 2004; 190:439–447. [PubMed: 15243915]
8. Veenemans J, et al. Effect of supplementation with zinc and other micronutrients on malaria in Tanzanian children: a randomised trial. *PLoS Med.* 2011; 8:e1001125. [PubMed: 22131908]
9. Sazawal S, et al. Effects of routine prophylactic supplementation with iron and folic acid on admission to hospital and mortality in preschool children in a high malaria transmission setting:

- community-based, randomised, placebo-controlled trial. *Lancet*. 2006; 367:133–143. [PubMed: 16413877]
10. Soofi S, et al. Effect of provision of daily zinc and iron with several micronutrients on growth and morbidity among young children in Pakistan: a cluster-randomised trial. *Lancet*. 2013; 382:29–40. [PubMed: 23602230]
 11. Portugal S, et al. Host-mediated regulation of superinfection in malaria. *Nat. Med.* 2011; 17:732–737. [PubMed: 21572427]
 12. Schümann K, et al. Impact of oral iron challenges on circulating nontransferrin-bound iron in healthy Guatemalan males. *Ann. Nutr. Metab.* 2012; 60:98–107. [PubMed: 22398912]
 13. Clark M, Fisher NC, Kasthuri R, Cerami Hand C. Parasite maturation and host serum iron influence the labile iron pool of erythrocyte stage *Plasmodium falciparum*. *Br. J. Haematol.* 2013; 161:262–269. [PubMed: 23398516]
 14. Bronzan RN, et al. Bacteremia in Malawian children with severe malaria: prevalence, etiology, HIV coinfection, and outcome. *J. Infect. Dis.* 2007; 195:895–904. [PubMed: 17299721]
 15. Berkley JA, et al. HIV infection, malnutrition, and invasive bacterial infection among children with severe malaria. *Clin. Infect. Dis.* 2009; 49:336–343. [PubMed: 19548833]
 16. Church J, Maitland K. Invasive bacterial co-infection in African children with *Plasmodium falciparum* malaria: a systematic review. *BMC. Med.* 2014; 12:31. [PubMed: 24548672]
 17. Lim C, et al. Expansion of host cellular niche can drive adaptation of a zoonotic malaria parasite to humans. *Nat. Commun.* 2013; 4:1638. [PubMed: 23535659]
 18. Chotivanich K, et al. Parasite multiplication potential and the severity of *falciparum* malaria. *J. Infect. Dis.* 2000; 181:1206–1209. [PubMed: 10720557]
 19. Cromer D, Stark J, Davenport MP. Low red cell production may protect against severe anemia during a malaria infection--insights from modeling. *J. Theor. Biol.* 2009; 257:533–542. [PubMed: 19168080]
 20. Pasvol G, Weatherall DJ, Wilson RJ. The increased susceptibility of young red cells to invasion by the malarial parasite *Plasmodium falciparum*. *Br. J. Haematol.* 1980; 45:285–295. [PubMed: 7002199]
 21. Tian LP, et al. Red cell age and susceptibility to malaria during pregnancy. *Acta. Obstet. Gynecol. Scand.* 1998; 77:717–721. [PubMed: 9740518]
 22. McQueen PG, McKenzie FE. Age-structured red blood cell susceptibility and the dynamics of malaria infections. *Proc. Natl Acad. Sci. USA.* 2004; 101:9161–9166.
 23. Bosch FH, et al. Characteristics of red blood cell populations fractionated with a combination of counterflow centrifugation and Percoll separation. *Blood.* 1992; 79:254–260. [PubMed: 1728314]
 24. Esposito A, et al. Quantitative imaging of human red blood cells infected with *Plasmodium falciparum*. *Biophys. J.* 2010; 99:953–960. [PubMed: 20682274]
 25. Bratosin D, Mitrofan L, Palii C, Estaquier J, Montreuil J. Novel fluorescence assay using calcein-AM for the determination of human erythrocyte viability and aging. *Cytometry A.* 2005; 66:78–84. [PubMed: 15915509]
 26. Tiffert T, et al. The hydration state of human red blood cells and their susceptibility to invasion by *Plasmodium falciparum*. *Blood.* 2005; 105:4853–4860. [PubMed: 15728121]
 27. Drakesmith H, Prentice AM. Hepsidin and the iron-infection axis. *Science.* 2012; 338:768–772. [PubMed: 23139325]
 28. Skaar EP. The battle for iron between bacterial pathogens and their vertebrate hosts. *PLoS Pathog.* 2010; 6:e1000949. [PubMed: 20711357]
 29. Jonker FAM, et al. Iron status predicts malaria risk in Malawian preschool children. *PLoS ONE.* 2012; 7:e42670. [PubMed: 22916146]
 30. Yip R, et al. Red cell membrane stiffness in iron deficiency. *Blood.* 1983; 62:99–106. [PubMed: 6860798]
 31. Yermiahu T, et al. Quantitative determinations of microcytic-hypochromic red blood cell population and glycerol permeability in iron-deficiency anemia and beta thalassemia minor. *Ann. Hematol.* 1999; 78:468–471. [PubMed: 10550558]

32. Brandão MM, et al. Impaired red cell deformability in iron deficient subjects. *Clin. Hemorheol. Microcirc.* 2009; 43:217–221. [PubMed: 19847056]
33. Bunyaratvej A, Butthep P, Sae-Ung N, Fucharoen S, Yuthavong Y. Reduced deformability of thalassemic erythrocytes and erythrocytes with abnormal hemoglobins and relation with susceptibility to *Plasmodium falciparum* invasion. *Blood.* 1992; 79:2460–2463. [PubMed: 1571557]
34. Goma J, Rénia L, Miltgen F, Mazier D. Iron overload increases hepatic development of *Plasmodium yoelii* in mice. *Parasitology.* 1996; 112(Pt 2):165–168. [PubMed: 8851855]
35. Koka S, et al. Iron deficiency influences the course of malaria in *Plasmodium berghei* infected mice. *Biochem. Biophys. Res. Commun.* 2007; 357:608–614. [PubMed: 17445762]
36. Matsuzaki-Moriya C, et al. A critical role for phagocytosis in resistance to malaria in iron-deficient mice. *Eur. J. Immunol.* 2011; 41:1365–1375. [PubMed: 21469097]
37. Zhao H, et al. Lipocalin 2 bolsters innate and adaptive immune responses to blood-stage malaria infection by reinforcing host iron metabolism. *Cell Host Microbe.* 2012; 12:705–716. [PubMed: 23159059]
38. Bei AK, et al. A flow cytometry-based assay for measuring invasion of red blood cells by *Plasmodium falciparum*. *Am. J. Hematol.* 2010; 85:234–237. [PubMed: 20196166]
39. Theron M, Hesketh RL, Subramanian S, Rayner JC. An adaptable two-color flow cytometric assay to quantitate the invasion of erythrocytes by *Plasmodium falciparum* parasites. *Cytometry A.* 2010; 77:1067–1074. [PubMed: 20872885]
40. Clark MA, et al. RBC Barcoding Allows for the Study of Erythrocyte Population Dynamics and *P. falciparum* Merozoite Invasion. *PloS One.* 2014; 9:e101041. [PubMed: 24984000]
41. Simpson JA, Silamut K, Chotivanich K, Pukrittayakamee S, White NJ. Red cell selectivity in malaria: a study of multiple-infected erythrocytes. *Trans. R. Soc. Trop. Med. Hyg.* 1999; 93:165–168. [PubMed: 10450440]
42. Sriprawat K, et al. Effective and cheap removal of leukocytes and platelets from *Plasmodium vivax* infected blood. *Malar. J.* 2009; 8:115. [PubMed: 19490618]

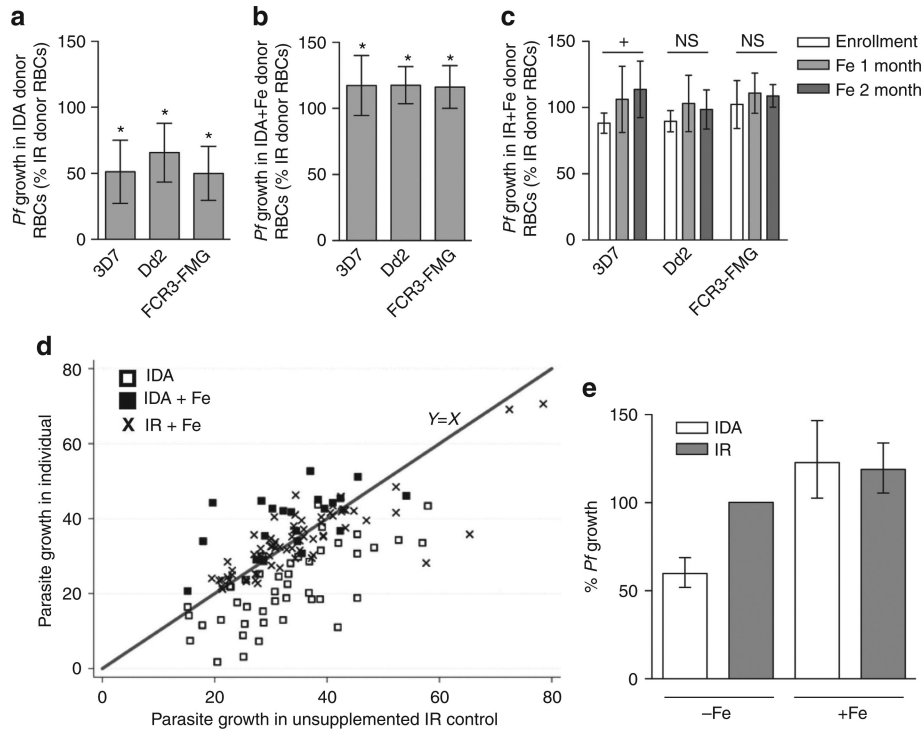


Figure 1. *P. falciparum* growth is reduced in iron-deficient RBCs and iron supplementation eliminates growth attenuation
(a–c) Growth experiments with RBCs from IDA donors ($n = 7$), IDA + Fe donors ($n = 5$) and IR + Fe donors ($n = 4$) were performed. Growth rate RBCs from an IR donor served as the control. Bars represent growth of *P. falciparum* (strains 3D7, Dd2 and FCR3-FMG) in indicated RBCs, normalized to growth in RBCs from IR donors (% Pf growth in IR RBC). Error bars represent the s.d. **(a)** Bars represent growth in RBCs from IDA donors. Significance was determined by two-tailed paired Student's *t*-test. * $P < 3 \times 10^{-10}$ as compared with *P. falciparum* growth in RBCs from IR donors. **(b)** Bars represent growth in RBCs from IDA + Fe donors. Significance was determined by two-tailed paired Student's *t*-test. * $P < 0.0003$ as compared with *P. falciparum* growth in RBCs from IR donors. **(c)** Bars represent growth of *P. falciparum* in RBCs from IR + Fe donors at enrollment, 1 month and 2 months on iron, normalized to growth in RBCs from IR donors (% Pf growth in IR RBC). Significance was determined by one-way analysis of variance. † $P < 0.02$ for strain 3D7 and nonsignificant (n.s.) for strains Dd2 and FCR3-FMG. **(d)** Mean growth rate of *P. falciparum* in RBCs from each individual IDA (□), IR + Fe (■) and IDA + Fe (×) donor plotted against the growth rate of *P. falciparum* in corresponding control RBCs from non-supplemented IR donors. Data were analysed by mixed effects regression. The $Y = X$ line was fit to the growth rates (in RBCs from IR donors). Points below the $Y = X$ line indicate growth rates less than that within RBCs from IR donors. **(e)** Graphical summary of the mixed effects regression analysis shown in **d**. Donor and parasite preparation were fitted as crossed random effects. The bars show the estimated parasite growth of *P. falciparum* in RBCs from the IDA, IDA + Fe and IR + Fe donors as a percent of *P. falciparum* growth in RBCs from non-supplemented IR donors. Error bars represent the 95% confidence interval.

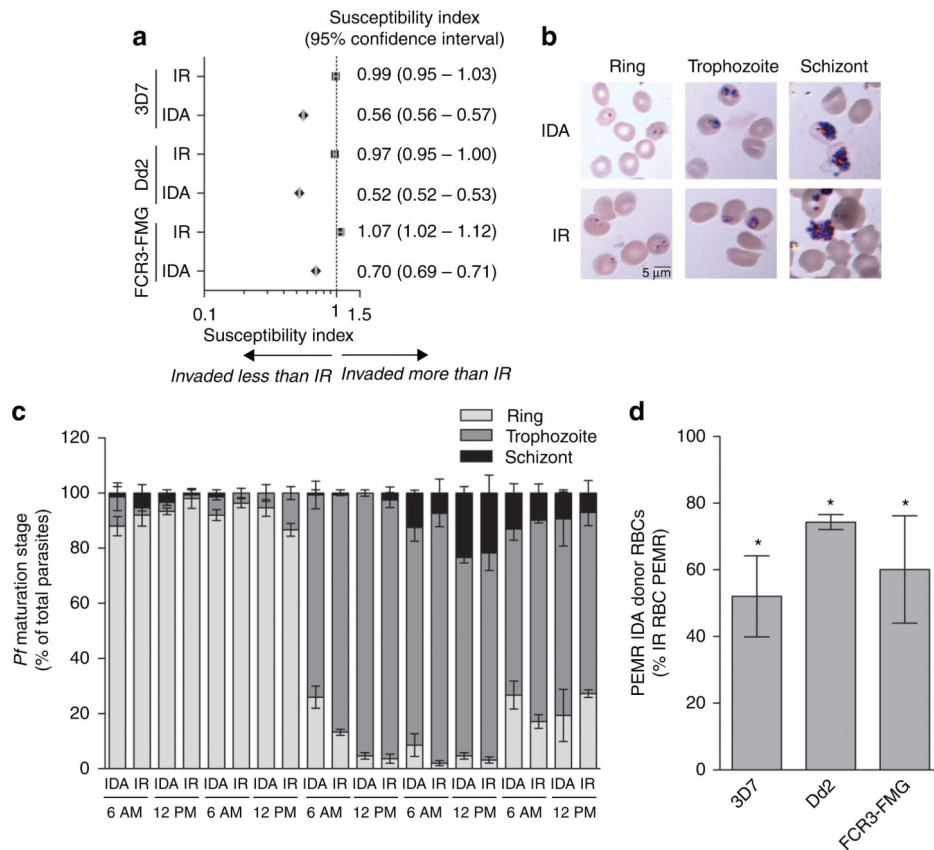


Figure 2. *P. falciparum* invasion and growth are reduced in RBCs from IDA donors
(a) Direct comparison of invasion into RBCs from either IDA or IR donors. Invasion experiments for RBCs from all IDA donors were performed independently and each experiment was performed in triplicate. Data show the mean SI of six independent experiments performed with RBCs from six IDA donors. The marker represents the SI point estimate and the bar represents the 95% CI. An SI of 1.0 indicates no difference in parasite invasion of the two RBC populations. **(b,c)** Comparison of the maturation of *P. falciparum* in RBCs donated by IDA and IR donors. Giemsa-stained thin blood smears were made every 6 h and 1,000 RBCs were counted by light microscopy to determine the percent of pRBCs as well as parasite intra-erythrocytic stage of maturation. Data are from a representative experiment (with strain FCR3-FMG) of three independent experiments performed with RBCs from three IDA donors infected with either *P. falciparum* strain 3D7, Dd2 or FCR3. **(b)** Giemsa-stained thin blood smears of *P. falciparum* ring, trophozoite and schizont stage parasites in RBCs from an IDA and an IR donor. **(c)** Bars indicate percent frequency of parasite ring, trophozoite and schizont stages in RBCs from an IDA and IR donor at each 6 h time point. Error bars represent the s.d. **(d)** Comparison of the parasite erythrocyte multiplication rate (PEMR) of *P. falciparum* within RBCs from IDA and IR donors. Bars represent PEMR of *P. falciparum* in RBCs from IDA donors, normalized to the PEMR of parasites in RBCs from IR donors (% IR PEMR). Data are the mean of three independent experiments performed in triplicate with RBCs from three IDA donors. Error bars represent the s.d. Significance determined by two-tailed paired Student's *t*-test. * $P < 3E^{-6}$, compared with PEMR in RBCs from IR donors.

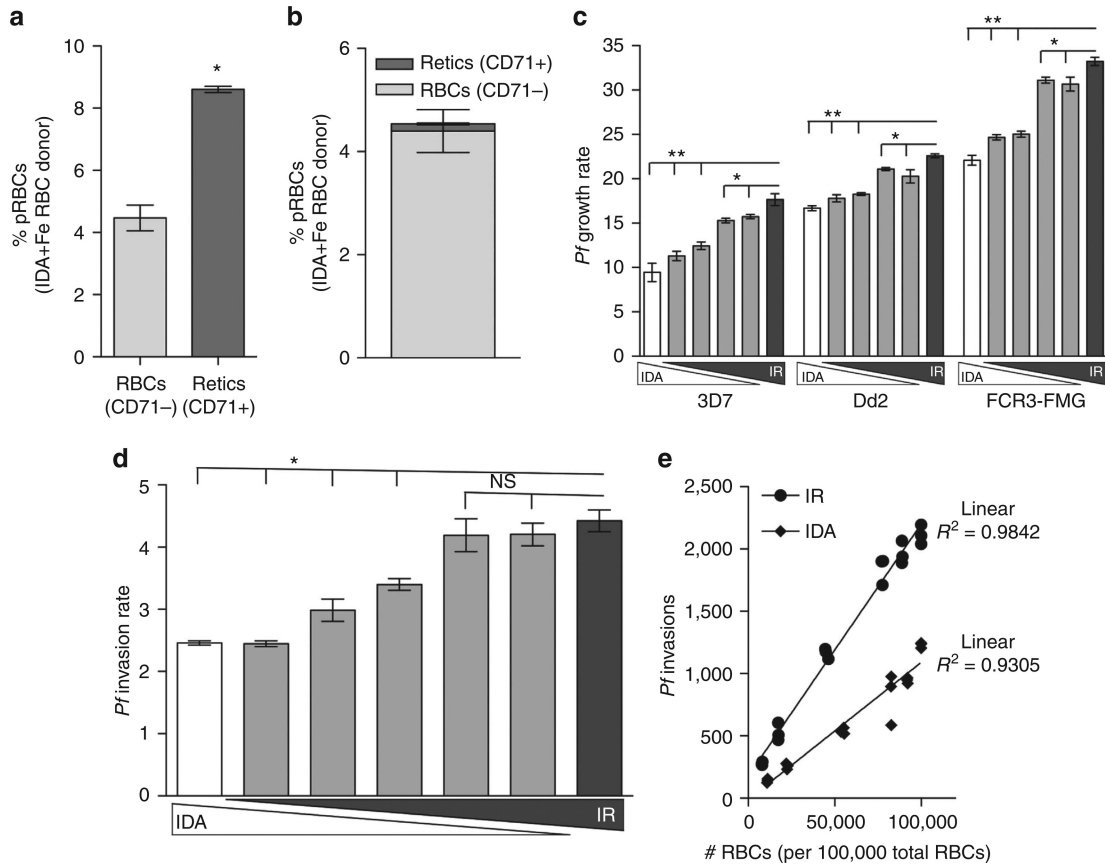


Figure 3. Replacement of iron-deficient RBCs with iron-replete RBCs increases *P. falciparum* infection

(a,b) *P. falciparum* (strain 3D7) infection of reticulocytes (CD71 +) and mature RBCs (CD71–) from an IDA + Fe donor. **(a)** Bars represent the percent of parasitized reticulocytes (CD71+) and mature RBCs (CD71–). Error bars represent the s.d. * $P < 0.0001$. **(b)** Contribution of parasitized reticulocytes (CD71+) and parasitized mature RBCs (CD71–) to the total infection. Error bars represent the standard deviation. **(c)** Growth rate of *P. falciparum* in RBC populations in which IDA RBCs were replaced with IR RBCs. RBCs were inoculated individually or together in the same wells at different ratios (100% IDA; 90% IDA and 10% IR; 75% IDA and 25% IR; 50% IDA and 50% IR; 25% IDA and 75% IR; 100% IR) and subsequently infected. Elongated triangles below the x axis represent the percentage of IDA RBCs (white triangle) and IR RBCs (grey triangle) in the total RBC population. Bars represent parasite growth rates after one 96 h growth assay. Error bars represent the s.d. * $P < 0.01$ and ** $P < 0.0003$. **(d and e)** Invasion rate of *P. falciparum* into RBC populations in which IDA RBCs were replaced with IR RBCs. Differentially labelled RBC donors were inoculated individually or together in the same wells at different ratios (100% IDA; 90% IDA and 10% IR; 80% IDA and 20% IR; 50% IDA and 50% IR; 20% IDA and 80% IR; 10% IDA and 90% IR; 100% IR). Each invasion condition contained 20×10^6 total RBCs. **(d)** Bars represent parasite invasion rate. Elongated triangles below the x axis represent the percentage of IDA RBCs (white triangle) and IR RBCs (grey triangle) in the total RBC population. Error bars represent the s.d. * $P < 0.001$, compared with *P.*

falciparum invasion rate into 100% IR RBCs. (e) Number of invasions events into IDA (diamonds) and IR (circles) RBCs as the frequency of each increases. Linear regression was used to determine the best fit lines for the data (IR $R^2 = 0.9842$ and IDA $R^2 = 0.9305$). Analysis of covariance was performed to compare the slopes of the lines and calculated $P < 0.0001$. The null hypothesis was no difference between the two RBC types ($H_0: \beta_{\text{Iron replete}} = \beta_{\text{Iron deficient}}$, $\alpha = 0.05$) n.s., nonsignificant.

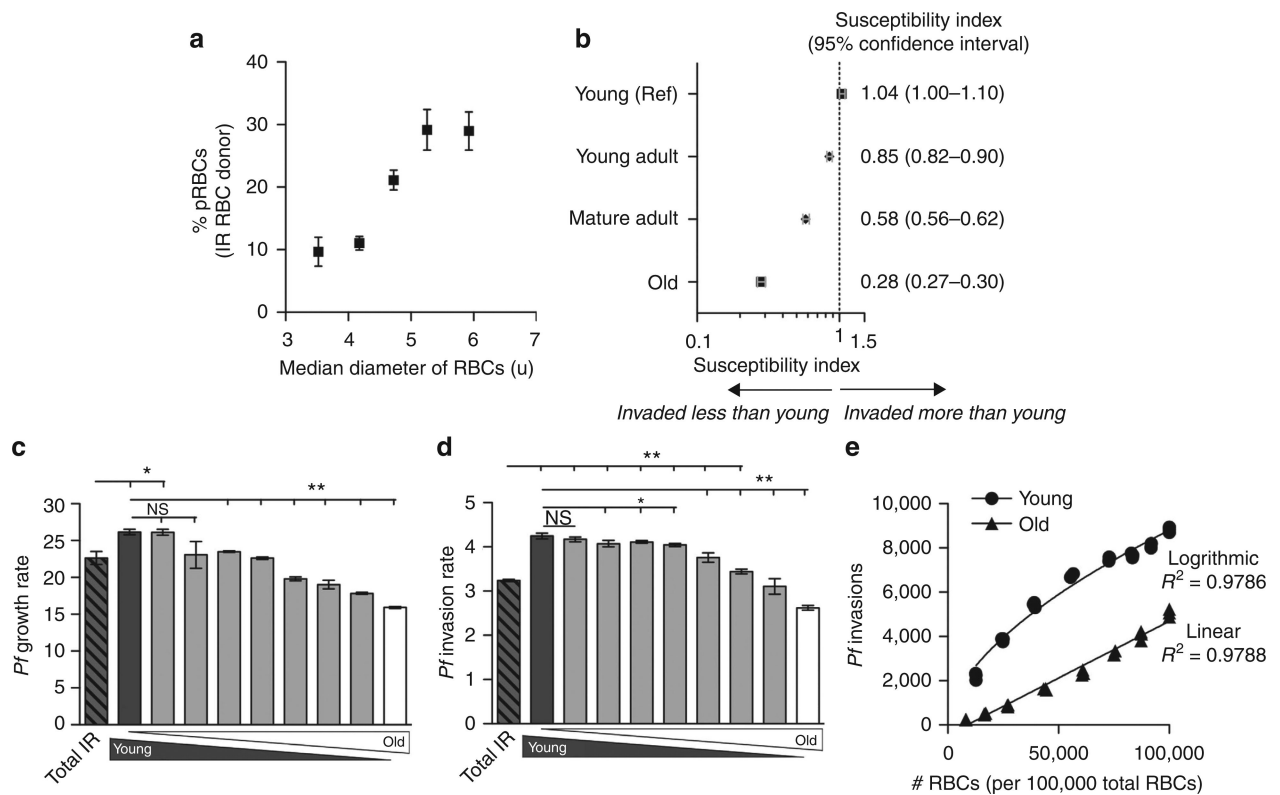


Figure 4. The elevated *P. falciparum* infection supported by young RBCs is reversed as young RBCs are replaced with old RBCs

(a) Percent *P. falciparum* (strain 3D7) infection of RBCs of increasing diameter. Data points represent the % pRBCs of five gated RBC populations of increasing volume. Error bars represent the s.d. (b) Direct comparison of *P. falciparum* (strain FCR3-FMG) invasion into RBCs of increasing age. IR RBCs were separated into five fractions of increasing density, a proxy for increasing RBC age (Supplementary Fig. 3a–d). The markers represent the SI point estimate and the bar represents the 95% CI. (c) Growth rate of *P. falciparum* (strain FCR3-FMG) in RBC populations in which young IR RBCs were replaced with old IR RBCs (0%, 10%, 20%, 33%, 50%, 66%, 80%, 90% and 100% replacement young RBCs with old RBCs). Elongated triangles represent the percentage of young IR RBCs (gray triangle) and old IR RBCs (white triangle) in the total RBC population. Bars represent parasite growth rates after 96 h. Error bars represent the s.d. * $P < 0.004$ and ** $P < 0.0003$, compared to growth rate in 100% total IR and 100% young RBCs respectively. (d and e) Invasion into RBC populations in which young IR RBCs were replaced with old IR RBCs. Differentially labelled young and old RBCs were inoculated individually or together in the same wells at different ratios (0%, 10%, 20%, 33%, 50%, 66%, 80%, 90% and 100% replacement young RBCs with old RBCs). (d) Bars represent invasion rates. Elongated triangles represent the percentage of young IR RBCs (gray triangle) and old IR RBCs (white triangle) in the total RBC population. Error bars represent the s.d. * $P < 0.05$ and ** $P < 0.003$ (e) Number of invasions events into young (circles) and old (triangles) RBCs as the frequency of each increases. Linear regression was used to determine best fit lines. A linear function best fit old RBC data ($R^2 = 0.9788$) and a logarithmic function best fit young RBC data ($R^2 = 0.9786$).

Analysis of covariance was performed to determine whether invasion data of old and young RBCs differed significantly, $P < 0.0001$. The null hypothesis was no difference between the two RBC types ($H_0: \beta_{\text{iron replete}} = \beta_{\text{iron deficient}}, \alpha 0.05$) n.s., nonsignificant.

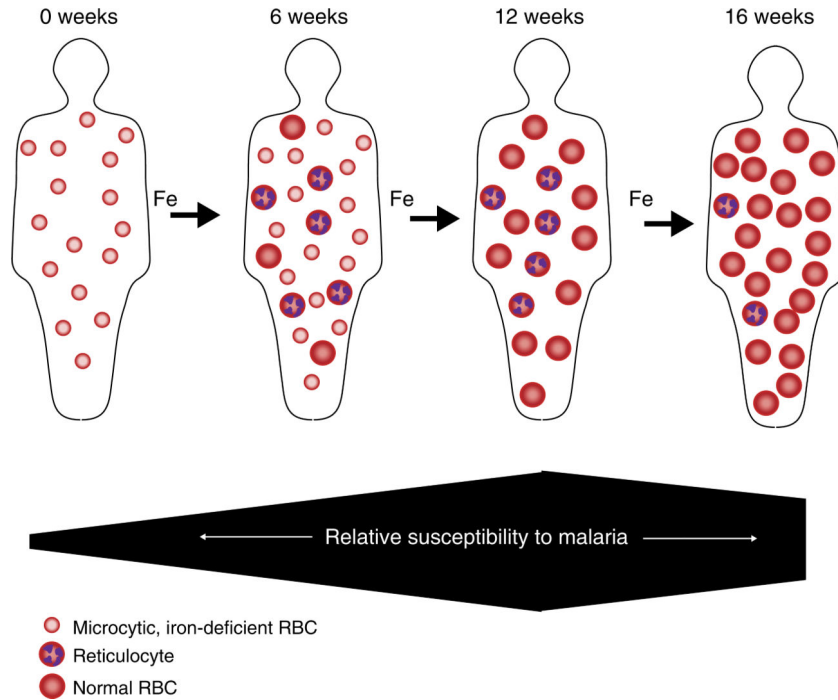


Figure 5. Hypothesized impact of iron deficiency and iron supplementation on host RBC population dynamics and susceptibility to erythrocytic stage malaria infection

Recovery from IDA is a complex process, which varies between individuals. Iron supplementation of an individual with IDA (0 weeks) will result in reticulocytosis and the production of young iron-replete RBCs (6 weeks). 12 weeks after the initiation of supplementation, the majority of the iron-deficient RBCs, will have been cleared from circulation (iron-deficient and iron-replete RBCs have 90 and 120 day lifespans respectively). After 16 weeks of iron supplementation, iron status has been corrected and the age structure of the RBC population will be restored. As shown above, we hypothesize that individuals with IDA will be less susceptible to erythrocytic stage malaria. The induction of erythropoiesis in these individual by iron supplementation and subsequent replacement of the iron-deficient RBCs with young iron-replete RBCs will increase the susceptibility of the individual to erythrocytic stage malaria infection. The susceptibility to infection is predicted to peak at the point when all iron-deficient RBCs have been replaced, but the age distribution of iron-replete RBCs is on average younger than a fully recovered iron-replete individual. Finally, restoration of the normal distribution of RBC age will return an individual's susceptibility to a normal level.

Table 1

Iron parameters and values of study participants.

Variable	Normal range	IDA (N = 7)	IDA + Fe (N = 6)	IR (N = 10)	IR after 1 month iron supplementation (IR + Fe; N = 4)	IR after 2 months iron supplementation (IR + Fe; N = 4)
White blood cell ($\times 10^9$ per l)	4.5-11.0	4.84 (1.78)	4.45 (1.15)	6.40 (1.61)	6.30 (1.41)	6.20 (1.12)
Red blood cell ($\times 10^{12}$ per l)	4.0-5.2	3.96 (0.60)	3.42 (0.35)	4.78 (0.52)	4.94 (0.52)	4.91 (0.39)
Haemoglobin (g dl ⁻¹)	12.0-16.0	8.20 (1.56)	8.73 (1.23)	14.60 (1.40)	14.90 (0.57)	14.63 (0.53)
Haematocrit (%)	36.0-46.0	28.13 (4.32)	29.11 (4.25)	42.80 (4.31)	43.85 (2.62)	42.88 (2.81)
Mean corpuscular volume (fL)	80.0-100.0	71.20 (6.63)	84.78 (8.28)	89.80 (2.74)	89.67 (4.24)	87.75 (2.50)
Mean corpuscular haemoglobin (Pg)	26.0-34.0	20.79 (2.54)	25.50 (2.35)	30.70 (0.95)	30.50 (2.12)	30.0 (1.83)
Mean corpuscular haemoglobin concentration (g dl ⁻¹)	31.0-37.0	29.20 (1.50)	30.27 (0.86)	34.20 (0.63)	34.50 (0.71)	34.25 (0.96)
Red cell distribution width (%)	12.0-15.0	17.41 (1.44)	18.13 (2.71)	13.22 (0.85)	13.90 (0.28)	13.20 (0.45)
Mean platelet volume (fL)	7.0-10.0	8.56 (1.05)	8.78 (0.65)	7.63 (0.54)	8.45 (0.92)	8.15 (0.52)
Platelet count ($\times 10^9$ per l)	150.0-440.0	294.57 (59.70)	344.0 (168.63)	251.80 (36.70)	212.50 (89.80)	256.0 (79.31)
Iron total (mg dl ⁻¹)	35.0-165.0	21.60 (10.55)	32.0 (16.79)	103.60 (43.34)	105.75 (32.71)	87.50 (17.99)
Transferrin (mg dl ⁻¹)	200.0-380.0	343.60 (74.72)	305.20 (63.55)	264.30 (41.33)	275.0 (29.50)	276.75 (31.83)
Transferrin iron binding capacity (mg dl ⁻¹)	252.0-479.0	438.67 (92.08)	384.60 (80.29)	333.0 (52.20)	346.0 (37.43)	348.75 (40.07)
Transferrin saturation (%)	15.0-50.0	4.71 (3.15)	8.0 (7.45)	31.60 (13.04)	31.0 (9.49)	25.75 (7.63)
Ferritin (ng ml ⁻¹)	30.0-151.0	5.71 (2.75)	17.17 (25.44)	42.01 (24.28)	46.75 (38.75)	33.33 (18.45)
Reticulocyte (%)	0.5-2.7	1.42 (0.55)	3.52 (1.62)	1.48 (0.48)	2.40 (0.71)	1.40 (0.38)

IDA, iron deficiency anaemia; IDA + Fe, iron deficiency anaemia on iron supplementation; IR, iron replete.

Tests were performed by McClendon Clinical Laboratory on samples taken from each donor at the same time points that blood samples were drawn for experiments. Values in the Normal Range column are the normal or healthy range for each parameter as defined by the McClendon Clinical Laboratory. Numerical values reflect the mean value of all individuals in each group and values in parentheses indicate standard deviation.